



## Characterization of planer cathode-supported SOFC prepared by a dual dry pressing method

Gang Chen<sup>a,\*</sup>, Hong-Xin You<sup>b</sup>, Yutaka Kasai<sup>c</sup>, Hiroyuki Sato<sup>a</sup>, Abuliti Abudula<sup>a,d,\*</sup>

<sup>a</sup> Faculty of Science and Technology, Hirosaki University, 1-bunkyocho, Hirosaki 036-8560 Japan

<sup>b</sup> Chemical Engineering College, Dalian University of Technology, No.2 Linggong Road, Dalian 116024, China

<sup>c</sup> Industrial Research Institute, Aomori Prefectural Industrial Technology Research Center, 4-11-6, Second Tonyamachi, Aomori 030-0113, Japan

<sup>d</sup> North Japan Research Institute for Sustainable Energy (NJRISE), Hirosaki University, 2-1-3, Matsubara, Aomori 030-0813, Japan

### ARTICLE INFO

#### Article history:

Received 2 July 2010

Received in revised form 2 October 2010

Accepted 6 October 2010

Available online 2 March 2011

#### Keywords:

Solid oxide fuel cell

Cathode-supported

Dry pressing

ScSZ

### ABSTRACT

Cathode-supported solid oxide fuel cells (SOFCs), comprising porous  $(\text{La}_{0.75}\text{Sr}_{0.25})_{0.95}\text{MnO}_{3-\delta}$  (LSM) +  $\text{Sm}_{0.2}\text{Ce}_{0.8}\text{O}_{1.9}$  (SDC) composite cathode substrate and 11 mol%  $\text{Sc}_2\text{O}_3$ -doped  $\text{ZrO}_2$  (ScSZ) electrolyte membranes layer, were successfully fabricated via dual dry pressing method. NiO-SDC anode was prepared by slurry coating method. Phase characterizations and microstructures of electrolyte and cathode were studied by X-ray diffraction (XRD) and scanning electronic microscopy (SEM). No interface reaction took place between LSM/SDC cathode substrate and ScSZ electrolyte layer after sintered at  $1300^\circ\text{C}$ . The cell performances were measured at 800 and  $750^\circ\text{C}$ , respectively, by changing the external load. The peak power densities were 0.228 and  $0.133\text{ W cm}^{-2}$ , and the corresponding open-circuit voltages of the cell were 1.092 and  $1.027\text{ V}$  at 800 and  $750^\circ\text{C}$ , respectively. Impedance analysis indicated that the performances of the SOFCs were determined essentially by the composition and microstructure of the electrode.

© 2011 Elsevier B.V. All rights reserved.

### 1. Introduction

Solid oxide fuel cell (SOFC) is a device that converts chemical energy into electric power through electrochemical reactions at elevated temperatures, which has been attracted more and more attention due to its high energy conversion efficiency, low emission and flexibility of fuels [1]. SOFC operating directly on hydrocarbon fuels without external reforming are expected to be an important technology for energy generation in the near future [2,3]. The state-of-the-art SOFC anode material, Ni/YSZ, has a number of disadvantages including Ni coarsening, sulfur poisoning, carbon deposition and redox instability [4]. In order to overcome these disadvantages, several alternative materials were investigated as potential anodes in recent years. Gorte et al. [5–8] avoided the problem of carbon deposition by using Cu– $\text{CeO}_2$  anode. Several authors have manifested that anodes based on a perovskite structure are promising candidates for future fuel cell anodes [9–12]. In theory, it may be hypothesised that the anode layer near the three phase boundary, close to the electrolyte membrane where the oxygen supply is more effective, is properly stabilized by the transported

oxygen ions. Thus, the anode layer should be sufficiently thin as in the present case. It has been previously evidenced that a reduction of the ohmic drop limitations appears necessary for increasing of the performance. A thin film electrolyte configuration would be a possible solution. This requires that a cathode-supported configuration is adopted. In any case, a cathode-supported SOFC with thin oxide-based anode layer would also, in principle, provide benefits in terms of tolerance to redox cycles for SOFC devices.

The low cost of LSM cathode supporting material is a big advantage of cathode-supported SOFC for the commercialization of SOFC [13]. But the formation of zirconate phases ( $\text{La}_2\text{Zr}_2\text{O}_7$  and  $\text{SrZrO}_3$ ) at the LSM and zirconia-based electrolyte interface is one of the most important degradation mechanisms [14]. In this study, in order to avoid the reaction between LSM cathode and zirconia-based electrolyte occurred above  $1300^\circ\text{C}$ , A-site deficient  $(\text{La}_{0.75}\text{Sr}_{0.25})_{0.95}\text{MnO}_{3-\delta}$  material, which has shown to be less reactive with zirconia based electrolyte than the stoichiometric one [1,15], was used.

To significantly reduce the cost of fabrication, dry pressing for fabrication of dense ceramic membranes on porous substrates was investigated. Compared with other methods such as physical or chemical vapor deposition for film preparation [16], dry pressing is simple, reproducible, and very cost-effective. In the present study, a thin ScSZ electrolyte film was prepared on a LSM–SDC cathode substrate and co-sintered to form a assembly.

\* Corresponding author. Tel.: +81 17 735 3362; fax: +81 17 735 5411.

E-mail addresses: [chen.1721@hotmail.com](mailto:chen.1721@hotmail.com) (G. Chen), [abuliti@cc.hirosaki-u.ac.jp](mailto:abuliti@cc.hirosaki-u.ac.jp) (A. Abudula).

## 2. Experimental

### 2.1. Fabrication of unit-cells

A samarium-doped cerium oxide (SDC,  $\text{Sm}_{0.2}\text{Ce}_{0.8}\text{O}_{1.9}$ ) powder was prepared by the sol-gel technique reported elsewhere [17]. Self-made SDC, LSM (CAS, China) and starch powders in a weight ratio of 3:1:1 were ball-milled in ethanol for 24 h, 5 wt% (relative to LSM+SDC) of polyvinyl butyral (PVB) was added and dispersed in ethanol by a magnetic stirring for 2 h and subsequently dried and ground with mortar and pestle, then passed through a 150  $\mu\text{m}$  mesh sieve. The mixed powder was pressed under 30 MPa into a substrate in a stainless-steel die. The Scandia stabilized zirconia (ScSZ, Tosoh Corporation, Japan) powder with 5 wt% PVB (relative to ScSZ) was added onto the substrate and co-pressed at 200 MPa to form an assembly. The assembly was subsequently sintered at 1300 °C for 4 h in air, and thus a dense, well-bonded electrolyte and cathode assembly was obtained. The thickness of the electrolyte film was controlled with the amount of ScSZ powder. The porosity of the cathode substrate was measured using a standard Archimedes method. NiO (Soekawa Chemicals, Japan)-SDC(self-made) powders in a weight ratio of 1:1 were also ball-milled in ethanol for 24 h, and prepared on electrolyte as anode by slurry coating method, which was then fired at 1300 °C in air for 2 h to form a porous anode. The effective anode area was 0.78  $\text{cm}^2$ .

### 2.2. Measurement

The cell performances were measured at 800 and 750 °C, respectively, by changing the external load. The current collector was Pt mesh. The anode was reduced with hydrogen for 20 min. The flow rates of  $\text{H}_2$  and  $\text{O}_2$  were both 100  $\text{ml min}^{-1}$ . The impedances were measured between 0.1 Hz and 1 MHz with excitation current of 0.001 A using a frequency response analyzer and a potentiostat (Solartron 1250B and 1286, respectively). The microstructure and morphology of the cells after testing were observed using scanning electron microscopy (SEM, Hitachi, S-800, Japan). To check the interface reaction between ScSZ film and LSM/SDC cathode substrate, the X-ray diffraction (XRD, Shimadzu, Japan) with  $\text{Cu K}\alpha$  radiation was used. To investigate shrinkage characteristics of the starting materials, the as-prepared powders with fixed weight were pressed to discs in 25.5 mm diameter by uniaxial dry pressing at 200 MPa. This was followed by sintering at selected temperatures in the range of 600–1300 °C with a heating rate of 3.3 °C  $\text{min}^{-1}$ . The dimensions of the unfired and sintered discs were measured to determine the shrinkage. The shrinkage of the discs was determined as  $(d_2 - d_1)/d_1$ , where  $d_1$  and  $d_2$  are initial and final diameter, respectively.

## 3. Results and discussion

Fig. 1 shows the XRD patterns of ScSZ and LSM composite powder sintered at different temperatures. The ScSZ and LSM composite powders were ball-milled in ethanol for 24 h with a weight ratio of 1:1, and then sintered at 1100, 1300 and 1350 °C for 2 h, respectively. No  $\text{La}_2\text{Zr}_2\text{O}_7$  or  $\text{SrZrO}_3$  was formed in any temperatures, indicating that the A-site deficient LSM can effectively prevent the formation of  $\text{La}_2\text{Zr}_2\text{O}_7$  or  $\text{SrZrO}_3$ . From this, it is reasonable to deduce that there were also no interface reaction taken place

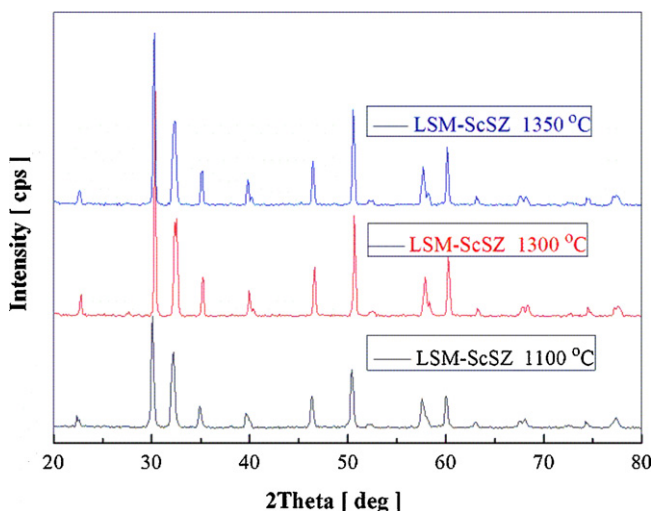


Fig. 1. XRD patterns of ScSZ and LSM composite powders sintered at 1100, 1300 and 1350 °C.

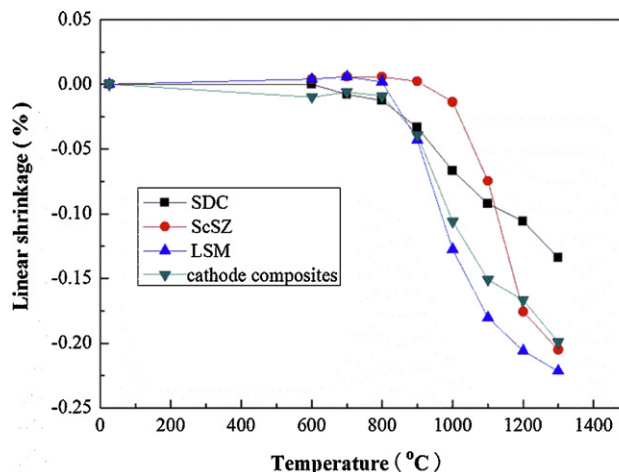


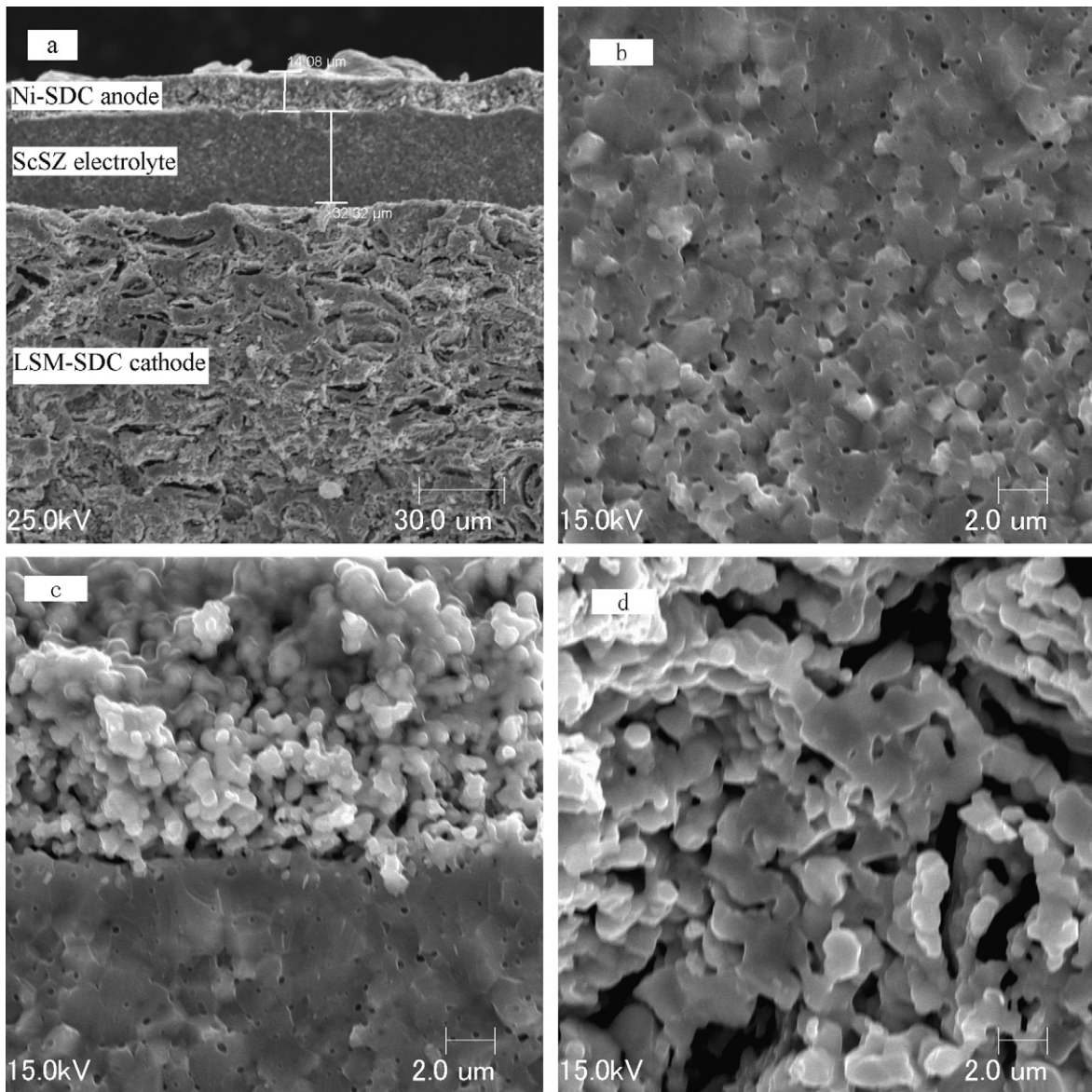
Fig. 2. Shrinkage ratio curves of SDC, ScSZ, LSM and cathode composite materials (LSM, SDC and starch powders in a weight ratio of 3:1:1 after ball-milled for 24 h).

between LSM/SDC cathode substrate and ScSZ electrolyte sintered at 1300 °C.

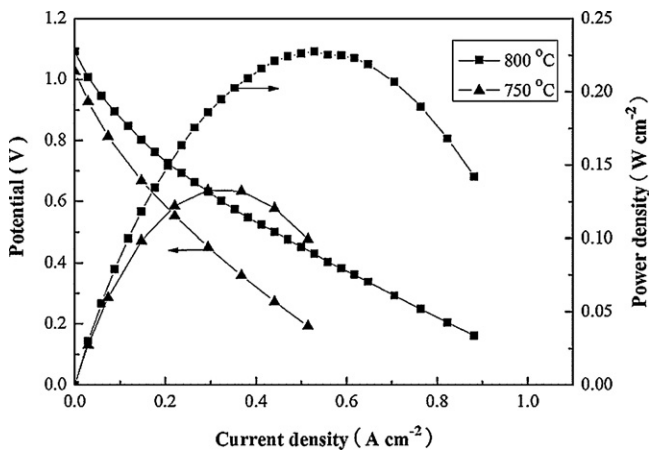
Fig. 2 shows the shrinkage ratio curves of SDC, ScSZ, LSM and cathode composite materials (LSM, SDC and starch powders in a weight ratio of 3:1:1 after ball-milled for 24 h). The shrinkages of SDC, ScSZ, LSM at 1300 °C were 13.3%, 20.5% and 22.2%, respectively. In order to make the cathode substrate have a similar shrinkage ratio with ScSZ electrolyte film at 1300 °C, and have no crack and warp in electrolyte and cathode assembly, SDC power and pore forming agent (starch) with certain ratio were added in LSM and ball-milled in ethanol for 24 h. As shown in Fig. 2, the supporting cathode dominated the shrinkage of the assembly at a temperature of below 1200 °C. At a temperature of above 1200 °C, the cathode substrate had similar shrinkage rate and shrinkage ratio with the ScSZ film. 4-h holding time at 1300 °C could assist the densification of electrolyte film.

Fig. 3 shows the cross-sectional scanning electron micrographs (SEM) of each cell component. Fig. 3(a) shows the overview of the sandwich structure of the whole cell. The thicknesses of cathode substrate, anode and electrolyte were 680, 14 and 32  $\mu\text{m}$ , respectively. Fig. 3(b) shows the high magnification of the ScSZ electrolyte film. Some isolated defects such as small voids were observed in electrolyte film. However, no cross-membrane cracks or pinholes were observed. The open-circuit voltages (OCVs) of the cell were 1.092 and 1.027 V at 800 and 750 °C, respectively, suggesting that the ScSZ layer was sufficiently dense to prohibit crossover of gases through the layer. Fig. 3(c) and (d) were high magnification of ScSZ layer and Ni-SDC anode and LSM-SDC cathode substrate, respectively. The electrodes showed typical porous microstructure. Porosity of the cathode substrate was about 30% determined by Archimedes method in water. The average grain sizes of the anode and cathode were approximately 0.5  $\mu\text{m}$  and 1.4  $\mu\text{m}$ , respectively.

Fig. 4 shows typical  $I$ - $V$  curves of the fuel cell at different temperatures. The peak power densities were 0.228 and 0.133  $\text{W cm}^{-2}$  at 800 and 750 °C, respectively. The corresponding OCVs of the cell were 1.092 and 1.027 V at 800 and 750 °C, respectively, which were close to the theoretical values predicted by Nernst equation [18]. This indicated that the ScSZ electrolyte film prepared by dual dry pressing method could meet the need of SOFC. The power densities were lower than those of the similarly-structured cathode-supported cell with Ni-SDC/YSZ-SDC/PNSM-SDC configuration at the same temperature [19]. The main reasons may be that the as-prepared cell had thicker electrolyte film, and greater grain size in cathode substrate.



**Fig. 3.** Cross-section of the cell, (a) overview of the sandwich structure of the whole cell, (b) high magnification of the electrolyte, (c) high magnification of the anode and electrolyte, and (d) high magnification of the cathode.



**Fig. 4.** The typical  $I$ - $V$  curves of the fuel cell with ScSZ electrolyte at different temperature.

Fig. 5 shows impedance spectroscopy measured under open circuit condition at different temperatures. The ac impedance is made up of both ohmic and electrode polarization resistances. The low frequency intercept corresponds to the total resistance of the cell. The high frequency intercept represents the ohmic resistance ( $R_0$ ), involving ionic resistance of the electrolyte, electronic resistance of the electrodes, and some contact resistance associated with interfaces [20]. The  $R_0$  values were 0.77 and 1.05  $\Omega \text{ cm}^2$  at 800 and 750  $^\circ\text{C}$ , respectively. The difference between the high frequency and low frequency intercepts represents the electrode polarization resistance ( $R_p$ ). The  $R_p$  values were about 1.34 and 2.6  $\Omega \text{ cm}^2$  at 800 and 750  $^\circ\text{C}$ , respectively. The ionic conductivity of ScSZ was estimated to be 0.1  $\text{S cm}^{-1}$  at 800  $^\circ\text{C}$  and 0.06  $\text{S cm}^{-1}$  at 750  $^\circ\text{C}$ , respectively [21]. The corresponding ohmic resistances of ScSZ electrolyte film were estimated to be 0.032  $\Omega \text{ cm}^2$  at 800  $^\circ\text{C}$  and 0.053  $\Omega \text{ cm}^2$  at 750  $^\circ\text{C}$ , based on a ScSZ layer thickness of 32  $\mu\text{m}$ , an electrode area of 0.78  $\text{cm}^2$ , which were much smaller than the experimental results of  $R_0$ . The main reasons for high  $R_0$  may be the much greater contact resistances between ScSZ electrolyte and cathode substrate, which could be greatly affected by the con-



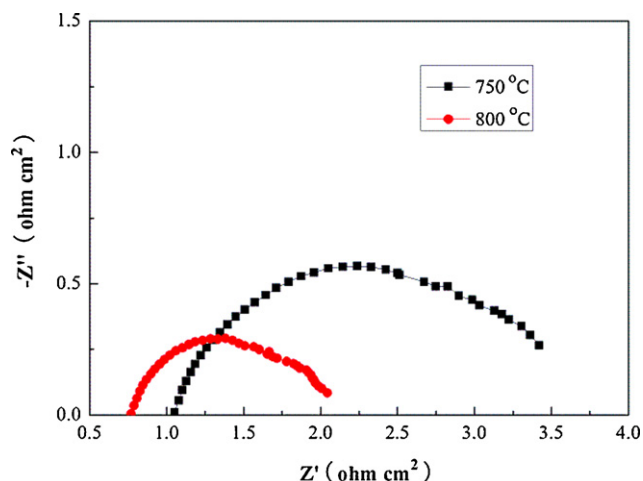


Fig. 5. Impedance spectra of the single cell measured under the open circuit state at 800 and 750 °C.

nective tightness between electrode and electrolyte. The higher contact resistances between ScSZ electrolyte and cathode substrate may be due to a little difference of shrinkage ratio between LSM–SDC cathode composite material and ScSZ electrolyte material in the process of co-sintering. As mentioned in some reference [19], the higher  $R_p$  resulted in a lower cell performance, especially at lower temperatures. As reported by Yamaguchi [22], an activation layer between cathode substrate and electrolyte obviously reduced the electrode polarization, indicating that the composition and microstructure of the electrode could be the main influencing factors of the electrical performance of the SOFC. In future, for further improvement of the electrical performance of the cathode-supported cell, optimization of the composition and microstructure of the cathode substrate should be a prerequisite way.

#### 4. Conclusions

LSM–SDC cathode supported SOFC was successfully fabricated via a cost-effective technique dual drying pressing method. A-site deficient LSM material successfully avoided the interface

reaction between LSM–SDC cathode and ScSZ electrolyte. The peak power densities were 0.228 and 0.133 W cm<sup>-2</sup> at 800 and 750 °C. The corresponding open-circuit voltages of the cell were 1.092 and 1.027 V at 800 and 750 °C, respectively. The OCV indicated that the ScSZ electrolyte film prepared by dual dry pressing method was dense enough. In summary, for further improvement of the cell performance, optimization of the composition and microstructure of the cathode substrate should be a prerequisite way. Future work will focus on improvement of the composition and microstructure of the cathode substrate in order to reduce the contact resistances and the electrode polarization.

#### Acknowledgements

This study was supported by the Go Go Foundation of Hirosaki University and by the State Scholarship Fund of China Scholarship Council (2008).

#### References

- [1] C. Zhao, R. Liu, S. Wang, *Electrochem. Commun.* 11 (2009) 842–845.
- [2] M.D. Gross, J.M. Vohs, R.J. Gorte, *Electrochim. Acta* 52 (2007) 1951–1957.
- [3] Y. Nabae, I. Yamanaka, *J. Electrochem. Soc.* 153 (1) (2006) A140–A145.
- [4] A. Atkinson, S. Barnett, R.J. Gorte, J.T.S. Irvine, *Nat. Mater.* 3 (2004) 17–27.
- [5] C. Lu, W.L. Worrell, J.M. Vohs, *J. Electrochem. Soc.* 150 (2003) A1357–A1359.
- [6] S. An, C. Lu, W.L. Worrell, R.J. Gorte, *Solid State Ionics* 175 (2004) 135–138.
- [7] R.J. Gorte, S. Park, J.M. Vohs, *Adv. Mater.* 12 (2000) 1465–1469.
- [8] O. Costa-Nunes, R.J. Gorte, *J. Power Sources* 141 (2005) 241–249.
- [9] S.W. Tao, J.S. Irvine, *Nat. Mater.* 2 (2003) 320–323.
- [10] S.W. Tao, J.T.S. Irvine, *Chem. Rec.* 4 (2004) 83–95.
- [11] B.A. Boukamp, *Nat. Mater.* 2 (2003) 294–296.
- [12] M.A. Raza, I.Z. Rahman, S. Beloshapkin, *J. Alloys Compd.* 485 (2009) 593–597.
- [13] M. Ippommatsu, H. Sasaki, S. Otoshi, *Int. J. Hydrogen Energy* 21 (2) (1996) 129–135.
- [14] A. Hagen, Y.L. Liu, R. Barfod, P.V. Hendriksen, *ECS Trans.* 7 (2007) 301–309.
- [15] S.P. Jiang, *J. Mater. Sci.* 43 (2008) 6799–6833.
- [16] J. Will, A. Mitterdorfer, C. Kleinlogel, D. Perednis, *Solid State Ionics* 131 (2000) 79–96.
- [17] A. Bodien, J. Di, C. Lagergren, *J. Power Sources* 172 (2007) 520–529.
- [18] S. McIntosh, *Electrochem. Solid-State Lett.* 6 (11) (2003) A240–A243.
- [19] M. Liu, D. Dong, F. Zhao, *J. Power Sources* 182 (2008) 585–588.
- [20] C. Zhao, R. Liu, S. Wang, *J. Power Sources* 192 (2009) 552–555.
- [21] C. Haering, A. Roosen, H. Schichl, M. Schnfller, *Solid State Ionics* 176 (2005) 261–268.
- [22] T. Yamaguchi, *J. Electrochem. Soc.* 155 (4) (2008) B423–B426.